Proton Magnetic Resonance Study of Nucleosides, Nucleotides, and Dideoxynucleoside Monophosphates Containing a *Syn* Pyrimidine Base

WALTER P. NIEMCZURA and FRANK E. HRUSKA, *Department of Chemistry, The University of Manitoba;* and KRISHNA L. SADANA and PETER C. LOEWEN, *Department of Microbiology, The University of Manitoba, Winnipeg, Manitoba, Canada R3T 2N2*

Synopsis

Proton magnetic resonance data have been obtained for 6-methyl-2′-deoxyuridine (dT*), its 3′- and 5′-monophosphates, and its 3′,5′-diphosphate, as well as for the corresponding thymine derivatives. The synthesis of the dideoxynucleoside monophosphates—d(TpT), d(T*pT), d(TpT*), and d(T*pT*)—was accomplished, and spectral data were obtained for these four dimers. The data show that the 6-methyluracil base prefers the *syn* conformation about the *N*-glycosyl bond at the monomer and dimer levels. The presence of the *syn* base leads to increases in the *cis* couplings of the sugar ring, $J_{1'2'}$ and $J_{2'3'}$, which indicate a trend towards eclipsing of the substituents on the C1′-C2′ and C2′-C3′ fragments. This trend is discussed in terms of changes in the pseudorotational parameters which describe the pucker of the ring. The *syn* base destabilizes the g^+ conformer about the C4′-C5′ bond, leading to a preference for the *t* conformer in all dT* residues at the monomer and dimer levels. Preliminary work on the formation of cyclobutane-type photodimers in d(T*pT) and d(T*pT*) is discussed and presented as evidence for the capability of the *syn* 6-methyluracil base to form base-stacked complexes.

INTRODUCTION

An important feature of nucleosides is the relative orientation of the base and sugar moieties, defined by the torsion angle χ, which falls into the *anti* and *syn* ranges. A new impetus to the study of the conformational consequences of the less common *syn* form is provided by the discovery of *syn* 2′-deoxyguanosine residues in left-handed double-helical DNA.[1,2] Though the *syn* conformation for pyrimidine residues is less favorable than for purines, experimental[3–11] and theoretical[12,13] data suggest that it might be found in special biological environments. For example, 4-thiouridine is found to crystallize in its *syn* form,[3] while a number of spectroscopic studies[4–10] have pointed to significant *syn* contributions to an *anti* $\rightleftarrows$ *syn* interconversion for pyrimidines in solution, at the monomer and oligomer levels. Hurd and Reid[11] have suggested the possibility of a *syn* pseudouridine residue in crystalline tRNA.

The photochemical studies of Ben-Hur and Ben-Ishai[14] may be providing

Biopolymers, Vol. 20, 1671–1690 (1981)

CCC 0006-3525/81/081671-20$02.00

indirect evidence for the presence of *syn* 2′-deoxythymidine residues in natural DNA. These authors have isolated from uv-irradiated, denatured DNA a minor thymine photodimer product in which the cyclobutane ring possesses the *TRANS–SYN* configuration. (Fully capitalized *CIS*, *SYN*, *TRANS*, and *ANTI* refer to the geometry of the cyclobutane ring[15]; lower-case *syn* and *anti* refer to the *N*-glycosyl conformation.) The major photodimer product, with the *CIS–SYN* cyclobutane geometry, would be formed most readily, it would seem,[16,17] from a d(TpT) fragment in a right-hand base-stacked conformation with both residues occupying their preferred *anti* conformations. Model building suggests that the *TRANS–SYN* photoproduct, on the other hand, would result from a right-handed base-stacked fragment with the 3′-linked residue rotated into its *syn* form, while the 5′-linked residue retains its *anti* form.

Useful model compounds for evaluating the conformational effects of *syn* pyrimidine bases are the 6-methyluracil derivatives, such as 6-methyl-2′-deoxyuridine (Fig. 1), since it is certain[18–25] that nucleosides so substituted are *syn*. Earlier we reported[24] the ^{1}H-nmr data of 6-methyl-

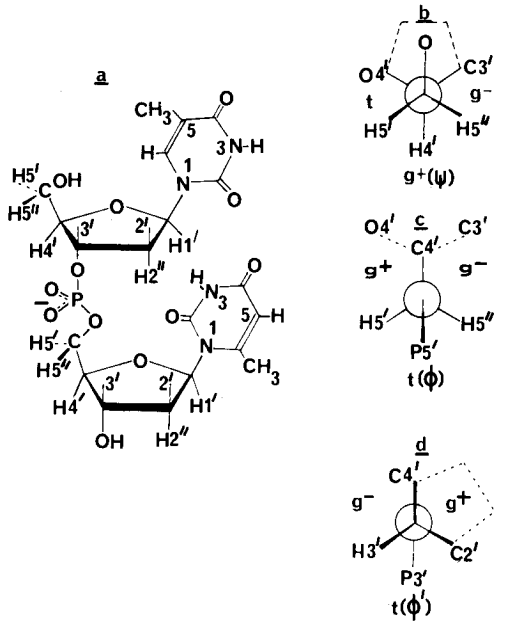

Fig. 1. (a) Structure of d(TpT*), a dideoxynucleoside monophosphate with a 3′-linked 2′-deoxythymidine (dT) and a 5′-linked 6-methyl-2′-deoxyuridine (dT*). The 3′-linked residue (Tp-) and the 5′-linked residue (-pT*) are shown in their *anti* and *syn* conformations, respectively. (b–d) Newman projections viewed along (b) C4′-C5′(ψ), (c) C5′-O5′(ϕ), and (d) C3′-O3′(ϕ'); g^+, t, and g^- refer respectively to the conformation domain containing the 60°, 180° (−180°), and 300° (−60°) conformer. (b) $g^+(\psi)$ conformer shown; t, g^- give location of O5′ in $t(\psi)$ and $g^-(\psi)$, respectively. (c) $t(\phi)$ conformer shown; g^+, g^- give location of P5′ in $g^+(\phi)$ and $g^-(\phi)$, respectively. (d) $t(\phi')$ conformer shown; g^+, g^- give location of P3′ in $g^+(\phi')$ and $g^-(\phi')$, respectively.

2′-deoxyuridine and 2′-deoxythymidine, and their 3′- and 5′-monophosphates, followed by a report[26] of the ^{13}C-^{31}P coupling constants of the monophosphates and the 3′,5′-diphosphates. To further our understanding of the conformational effects of *syn* pyrimidine bases, we extend here our proton ^1H-nmr study to the 3′,5′-diphosphates of 2′-deoxythymidine and 6-methyl-2′-deoxyuridine and to the 3′,5′-dideoxynucleoside monophosphates, d(TpT), d(TpT*), d(T*pT), and d(T*pT*). For simplifying the representation of these molecules, we shall use the following abbreviations: dT*, 3′dT*MP, 5′dT*MP, and dpT*p for 6-methyl-2′-deoxyuridine, and its 3′- and 5′-monophosphates and 3′,5′-diphosphates, respectively. The corresponding thymine molecules are dT, 3′dTMP, 5′dTMP, and dpTp. A 3′,5′-dideoxynucleoside monophosphate with a 3′-linked dT and 5′-linked dT* is d(TpT*), etc. (Fig. 1). The 3′- and 5′-linked fragments of d(TpT*) are Tp- and -pT*, respectively.

EXPERIMENTAL

Materials

The monomers dT, 3′dTMP, and 5′dTMP were purchased from the Sigma Chemical Company. dT* was prepared according to Holy.[27,28] In our hands, however, condensation of the starting material, 2-amino-β-D-arabinofuro (1′2′:4,5) oxazoline, with ethyl-β-chlorocrotonate in place of ethyl-2-butynoate[27] gave better yields. We also found that the completion of the benzoylation step required 2.5 h, and that acid hydrolysis of the anhydro linkage for 3 h increased the yield to 95% (58% reported[27,28] for 1-h hydrolysis). The monophosphates 3′dT*MP and 5′dT*MP were prepared according to George et al.[24] The 3′,5′-diphosphates, dpTp and dpT*p, were prepared by phosphorylating the unprotected nucleosides.

The dinucleoside monophosphates were prepared using the triester approach. The 5′-hydroxyl was protected by a monomethoxytrityl group in the case of dT and the trityl group for dT*. The 3′-hydroxyls were protected by the benzoyl group. Arylsulphonyltetrazoles were used as condensing agents for the formation of the 3′,5′-linkage, as suggested by Stawinski et al.[29]

NMR Spectral Data

All samples were examined in 5-mm (o.d.) tubes, at concentrations of 4 mg/ml in D_2O containing 0.1 mg sodium 3′-trimethylsilylpropionate-2,2,3,3-d_4 (TSP) as internal reference. Paramagnetic ions were removed by chromatography on Chelex-100 (Bio-Rad Laboratories) and by treatment with dithizone (J.T. Baker Chemical Co.) as described by Cozzone and Jardetzky.[30] The pH was adjusted by addition of dilute NaOD or DCl and is given in the tables as the pH meter reading. (A correction of 0.4 units should be added to the pH values to correct for the deuterium isotope ef-

fect.[31]) The samples were freeze-dried three times and dissolved in 100% D_2O (Aldrich Chemical Co).

The proton spectra were obtained on a Nicolet NT 360 Fourier transform spectrometer at the Purdue Biological Magnetic Resonance Laboratory (West Lafayette, Indiana). Spectral widths were typically 2400 Hz, acquired, with quadrature detection, into 32K data points of memory. Temperatures were maintained within ±1°C. Spectral analysis was carried out using LAME,[32] and computer-simulated spectra were generated as a final test of the data. All details of spectral acquisition (as well as synthesis) have been described in the Ph.D. thesis of W.P.N.[33] ^{1}H-nmr spectra were also obtained at 270 MHz (Biochemistry Department, University of Wisconsin, Madison) and 600 MHz (The University of Pittsburgh). ^{31}P spectra at 36.4 MHz (Bruker WH-90DS, The University of Manitoba) were useful for determining ^{31}P-^{1}H coupling constants. The uncertainties in the chemical shifts (δ) and coupling constants (J) are estimated to be about ±0.001 ppm and ±0.1 Hz, respectively. A portion of the 600-MHz spectrum of d(T*pT*) is shown in Fig. 2 accompanied by a simulated spectra.

Spectral Assignments

The assignment of the proton spectra has been provided for dT[34] and dT*[24] and their monophosphates, facilitating the assignments of the 3′,5′-diphosphate spectra. The dimer assignments were initiated by

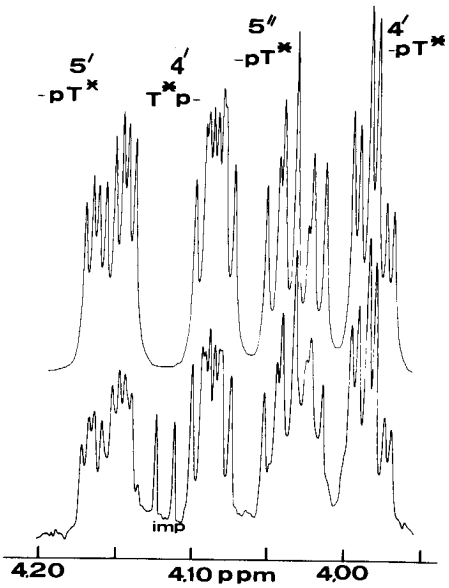

Fig. 2. Bottom trace: Pmr spectrum (600 MHz) of 3.95–4.20-ppm region of d(T*pT*) (relative to TSP). Conditions: 5 mg/ml, pH 6.5, 20°C. Impurity peaks at 4.11 and 4.13 ppm. Top: Computer-simulated spectrum.

comparison with the monomer spectra and with published assignments for various oligonucleotides.[34–40] Consideration of phosphorylation effects[41] and the presence of ^{1}H -^{31}P couplings aided in distinguishing between the H3′ protons of the 3′- and 5′-residues of the dimers. Proton-decoupling experiments enabled assignments of the remaining bands to be made, to one or the other of the residues. ^{1}H-decoupling of the H3′ bands provided assignments of the H2′, H2″, and H4′ bands to a particular residue. ^{1}H-decoupling of the H2′ and H2″ bands provided assignments for the H1′ bands. The distinction between the H2′ and H2″ on the same residue was based on coupling-constant arguments[36,37] which follow from selective-deuteration studies.[42] The H5′ and H5″ assignments followed from arguments by Remin and Shugar[43] and the selective-deuteration studies of Ritchie and Perlin.[44] When H2′ and H2″ are isochronous, only the averages $(J_{1'2'} + J_{1'2''})/2$ and $(J_{2'3'} + J_{2''3'})/2$ can be obtained from spectral analysis.

RESULTS

Table I lists the ^{1}H chemical shifts (ppm relative to internal TSP) of the nonexchangeable base and sugar protons of the 3′,5′-diphosphates and the four dinucleoside monophosphates. Data for dpTp and dpT*p (20°C) were obtained at pH values below and above the secondary phosphate ionization constant (≈6.2).[30] Data for d(TpT*) and d(T*pT) were obtained at 20 and 60°C, but due to time limitations on the 360-MHz spectrometer use, only 20°C data could be obtained for d(TpT) and d(T*pT*).

Table II lists the couplings $J_{1'2'}$ through $J_{3'4'}$ required for the discussion of the sugar pucker. The sums $(J_{1'2'} + J_{3'4'})$ and $(J_{1'2'} + J_{1'2''})$ are also given, the latter being useful when H2′ and H2″ are isochronous and the individual couplings unattainable.

Table III contains the couplings involving H4′, H5′, H5″, and P5′ required for the analysis of the ψ and ϕ conformer problem (Fig. 1). Also included are the H3′-P3′ couplings related to the ϕ' bond orientation. The four-bond couplings between the base methyl and H5 (or H6) protons are not listed (~1.1 and ~0.8 Hz for the thymine and 6-methyluracil base, respectively).

Our data for d(TpT) are in reasonable agreement with earlier studies at lower fields (220 and 270 MHz, Refs. 36 and 39, respectively).

DISCUSSION

Conformation About the *N*-Glycosyl Bond

Birnbaum and coworkers[19] have shown that crystalline dT* favors the *syn* form in contrast with dT, which is *anti*.[45] In solution, a qualitative approach to the *syn–anti* problem is based on the magnetic deshielding influence (0.5–0.6 ppm) of the 2-keto oxygen of a *syn*-pyrimidine base on

TABLE I

Chemical Shifts (δ, in ppm[a]) of the Nonexchangeable Base and Sugar Protons of dpTp, dpT*p, d(TpT), d(T*pT), d(TpT*), and d(T*pT*)[b]

	dpTp		dpT*p		d(TpT)		d(TpT*)				d(T*pT)					
							Tp-		-pT*		T*p-		-pT		d(T*pT*)	
Proton	pH 4.5	7.3	pH 3.7	7.5	Tp-	-pT	20°C	60°C	20°C	60°C	20°C	60°C	20°C	60°C	T*p-	-pT*
1′	6.403	6.387	6.265	6.252	6.188	6.300	6.250	6.247	6.189	6.197	6.175	6.160	6.335	6.307	6.156	6.194
2′	2.418	2.403	3.036	3.010	2.331	2.452	2.227	2.320	2.954	2.925	2.955	2.967	2.416	2.396	2.930	2.941
2″	2.544	2.502	2.477	2.436	2.541	2.452	2.416	2.476	2.311	2.318	2.436	2.424	2.416	2.397	2.463	2.292
3′	4.893	4.775	—	—	4.748	4.574	4.761	4.781	4.540	4.573	—	4.835	4.568	4.551	—	4.656
4′	4.377	4.310	4.182	4.130	4.163	4.106	4.130	4.166	4.022	4.043	4.056	4.066	4.156	4.150	4.086	3.984
5′	4.117	4.008	4.196	4.123	3.807	4.130	3.837	3.855	4.126	4.151	3.878	3.866	4.122	4.116	3.833	4.153
5″	4.117	4.008	4.049	3.961	3.759	4.059	3.762	3.782	3.981	4.030	3.734	3.746	4.053	4.058	3.731	4.034
5	—	—	5.722	5.718	—	—	—	—	5.560	5.628	5.704	5.709	—	—	5.719	5.646
6	7.800	7.858	—	—	7.665	7.654	7.555	7.560	—	—	—	—	7.704	7.665	—	—
CH_3	1.936	1.940	2.405	2.415	1.869	1.860	1.893	1.899	2.350	2.367	2.363	2.362	1.907	1.912	2.379	2.367

[a] From internal TSP.

[b] At 360.061 MHz; sample concentration, 4.0 mg/ml. Conditions: t = 20°C at pH 6.5 unless otherwise indicated.

TABLE II

^1H–^1H Coupling Constants (Hz) for a Series of dT and dT* Derivatives in Aqueous Solution, Required for Discussion of the Sugar Ring Pucker[a,b]

Molecule	Temp. (°C)	pH	*TRANS* $J_{1'2'}$	$J_{2''3'}$	$J_{3'4'}$	$J_{1'2'}+J_{3'4'}$	*CIS* $J_{1'2''}$	$J_{2'3'}$	$J_{1'2'}+J_{1'2''}$	Geminal,[c] $J_{2'2''}$
dT Residues										
dT	30	6.5	6.8	4.1	4.1	10.9	6.8	6.6	13.6	14.0
3′dTMP	30	5.4	7.2	3.7	4.0	10.7	6.5	6.8	13.7	14.3
5′dTMP	20	5.5	7.6	2.6	3.0	10.6	6.2	6.8	13.8	13.8
d(pTp)	20	4.5	8.2	2.4	2.4	10.6	6.0	6.1	14.2	14.1
	20	7.3	8.2	2.4	2.4	10.6	6.1	5.9	14.3	13.9
d(TpT)	20	6.5	6.7	3.6	3.6	10.3	6.5	7.0	13.4	14.1
d(T pT*)	20	6.5	7.0	3.6	4.2	11.2	6.8	7.1	13.8	14.2
	60	6.5	7.1	3.7	3.6	10.8	6.8	7.3	13.9	14.2
d(TpT)	20	6.5	—	—	3.5	—	—	—	13.7	—
d(T*pT)[d]	20	6.5	—	—	4.2	—	—	—	13.6	—
	60	6.5	—	—	3.7	—	—	—	13.6	—
dT* Residues										
dT*	30	6.5	5.3	5.5	5.9	11.2	8.4	8.3	13.7	13.9
3′dT*MP	18	6.0	5.6	5.2	5.8	11.4	8.2	8.1	13.8	13.8
5′dT*MP	25	6.0	4.7	6.1	6.1	10.8	8.5	8.4	13.2	13.9
d(pT*p)	20	3.7	4.9	5.6	6.1	10.5	8.7	8.4	13.6	14.0
	20	7.5	5.4	5.6	5.8	11.2	8.5	8.3	13.9	13.8
d(T*pT)	20	6.5	5.4	5.6	5.5	10.9	8.4	8.5	13.8	14.0
	60	6.5	5.7	5.1	5.3	11.0	8.3	7.9	14.0	13.9
d(T*pT*)	20	6.5	6.4	4.9	4.8	11.2	7.8	7.4	13.9	13.9
d(TpT*)	20	6.5	3.7	6.8	7.1	10.7	9.2	9.0	12.9	14.0
	60	6.5	4.3	6.2	6.5	10.8	8.4	8.7	12.7	14.1
d(T*pT*)[d]	20	6.5	4.0	6.6	6.9	10.9	9.1	8.9	13.1	13.7

[a] Data at 360 MHz except T*p- of d(T*pT*) (600 MHz). Data for dT, dT*, 3′dTMP, 3′-dT*MP, 5′dTMP (220 MHz), and 5′dT*MP (360 MHz) from Ref. 24.

[b] Estimated error, ±0.2 Hz.

[c] Negative.

[d] Dimer data refer to underlined residue.

H2′ of the sugar[46] and has been applied to dT* and its monophosphates.[24] To consider this problem for the 3′,5′-diphosphates and the dinucleoside monophosphates, we have calculated $\Delta\delta$ for H2′ as well as H2″ and H3′ using the data in Table I (see Table IV). $\Delta\delta$ is defined as the chemical shift of a proton in a dT* residue relative to its resonant position in the corresponding dT residue. For example, $\Delta\delta$(H2′) in Tp*- of d(T*pT) is the shift of this proton relative to H2′ in the Tp- residue of d(TpT). Thus, $\Delta\delta$ is a measure of the shift change experienced when the base on the same residue changes from *anti* to *syn*. For comparison, $\Delta\delta$ values for dT*, 3′dT*MP, and 5′dT*MP have been included (Ref. 24).

The $\Delta\delta$(H2′) data reveal a similarity in the influence of the T* base on the H2′ protons of the monomers, including the 3′,5′-diphosphate at the

TABLE III
Coupling Constants (Hz) for a Series of dT and dT* Derivatives Necessary for Discussion of the ψ(C4′-C5′), ϕ(C5′-O5′), and ϕ'(C3′-O3′) Conformations[a]

Molecule	Temp. (°C)	pH	$J_{4'5'}$	$J_{4'5''}$	Σ[c]	$J_{5'5''}$[d]	$J_{5'P}$	$J_{5''P}$	Σ'[c]	$J_{4'P}$	$J_{3'P}$
dT Residues[b]											
dT	30	6.5	3.6	5.0	8.6	12.4	—	—	—	—	—
3′dTMP	30	5.4	3.5	4.8	8.3	12.5	—	—	—	—	7.8
5′dTMP	30	5.4	—	—	7.6	—	—	—	10.0	1.6	—
d(pTp)	20	4.5	—	—	5.8	—	—	—	9.1	2.4	7.9
	20	7.3	—	—	5.6	—	—	—	8.0	1.0	8.3
d(TpT)	20	6.5	3.7	4.2	7.9	12.6	—	—	—	—	6.3
d(TpT*)	20	6.5	2.8	4.6	7.4	12.6	—	—	—	—	7.6
	60	6.5	3.3	4.7	8.0	12.6	—	—	—	—	7.0
d(TpT)	20	6.5	2.3	3.7	6.0	11.9	4.1	3.6	7.7	1.5	—
d(T*pT)	20	6.5	2.9	4.4	7.3	11.5	3.9	4.0	7.9	1.9	—
	60	6.5	3.1	4.7	7.8	11.5	4.4	5.1	9.5	1.4	—
dT* Residues[b]											
dT*	30	6.5	3.4	6.5	9.9	12.1	—	—	—	—	—
3′dT*MP	18	6.0	3.9	6.1	10.0	12.1	—	—	—	—	7.1
5′dT*MP	25	6.0	4.3	6.3	10.6	11.1	5.8	5.7	11.5	~0	—
d(pT*p)	20	3.7	3.4	7.5	10.9	11.4	6.3	6.3	12.6	~0	7.9
	20	7.5	3.3	7.9	11.2	11.6	5.8	5.7	11.5	~0	9.8
d(T*pT)	20	6.5	3.2	6.8	10.0	12.1	—	—	—	—	6.8
	60	6.5	3.5	6.5	10.0	12.1	—	—	—	—	7.4
d(T*pT*)	20	6.5	3.6	6.6	10.1	12.1	—	—	—	—	9.5
d(TpT*)	20	6.5	2.6	8.3	10.9	10.9	3.4	5.6	9.0	~0	—
	60	6.5	3.0	8.0	11.0	10.7	4.8	6.0	10.8	~0	—
d(T*pT*)	20	6.5	2.7	6.6	9.3	11.3	4.9	4.8	9.7	~0	—

[a] Data for dT(T*), 3′dT(T*)MP, and 5′dT(T*)MP, from Ref. 24.
[b] For dimers, relevant residue is underlined.
[c] $\Sigma = J_{4'5'} + J_{4'5''}$; $\Sigma' = J_{5'P} + J_{5''P}$
[d] Negative.
[e] Estimated error ±0.2 Hz.

two pH values (deshielding, 0.57–0.62 ppm). H2″ and H3′ experience much smaller effects, 0.07–0.12 ppm (shielding) and 0.01–0.06 ppm (deshielding), respectively. The general trends in $\Delta\delta$ for the dimer residues parallel those for the monomers, indicating that the preference for the *syn* conformation is retained by the T* base at the dimer level.

There are, however, some differences in the trends of the monomer and dimer levels. Thus, the $\Delta\delta$(H2′) dimer data define a somewhat larger range (0.50–0.70 ppm). Also, the values of $\Delta\delta$(H2′) are larger for the 3′-linked Tp*- residues (0.62–0.70 ppm) than for the 5′-linked -pT* residues (0.50–0.55 ppm). And noteworthy is the small, negative $\Delta\delta$(H3′) for Tp*- of d(T*pT*), which contrasts with the positive $\Delta\delta$(H3′) observed for all other entries in Table IV. These small differences in the general trends may be due to differences in the χ angle within the *syn* range of the T* bases and to differences in the pucker of the sugars, but they are not easily considered on a quantitative basis.

$\approx J_{2''3'} \approx J_{3'4'}$). In the literature one finds various methods for estimating N and S percentages. Care must be taken in comparing such data for, in particular, molecules in the *syn* series, on the one hand, and molecules in the *anti* series, on the other, since the limiting J values are certainly different for the two series. However, gross conformational *trends* are undoubtedly well defined by the calculated populations, since they are simply the trends in the couplings disguised by the arithmetical manipulation.

Dinucleoside Monophosphates

The general trends in the coupling constants of the Tp- and -pT residues of the dimers parallel those of the 3′- and 5′-monophosphates. The *cis* couplings in the Tp- units of d(TpT) and d(TpT*) lie in the range 6.5–7.3 Hz (6.5–6.8 Hz in 3′dTMP). The *cis* couplings in the -pT units could not be determined since H2′ and H2″ are isochronous, even at 600.2 MHz. The %S population, calculated from $J_{3'4'}$ by interpolation[50] (1 Hz in S; 10 Hz in N), lies in the range 64–78% for 3′dTMP, 5′dTMP, and the Tp- and -pT units. A slightly larger value (84%) is obtained for dpTp.

Like the T* monomers, the T*p- and -pT* units of the dimers show larger *cis* couplings than the corresponding T units. $J_{1'2''}$ and $J_{2'3'}$ are particularly large in the -pT* units of d(TpT*) and d(T*pT*) (8.9–9.2 Hz at 20°C). To the best of our knowledge these are the largest *cis* couplings observed to date in a 2′-deoxyribose ring, and they indicate the greatest restriction to torsional motion about the C1′-C2′ and C2′-C3′ bonds. At 60°C the *cis* couplings of d(TpT*) are reduced to 8.4 Hz ($J_{1'2''}$) and 8.7 Hz ($J_{2'3'}$). The *cis* couplings are somewhat smaller in the T*p- units of d(T*pT) and d(T*pT*). They lie in the range 7.9–8.5 Hz, except for $J_{2'3'}$ (7.4 Hz) in T*p- of d(T*pT*). This indicates that the trend towards eclipsing of the C1′-C2′ and C2′-C3′ substituents is not as pronounced in the 3′-linked units. Following the reasoning in the previous section, we account for the larger *cis* couplings with an N ⇄ S model in which both the N and S states have pseudorotated towards O4′-*endo*, relative to the thymine derivatives. A more pronounced shift to O4′-*endo* in the -pT* units is suggested by their larger *cis* couplings.

The *trans* couplings of the Tp*- and -pT* units show the trends seen at the monomer level, namely, decreases in $J_{1'2'}$ and comparable increases in $J_{2''3'}$ and $J_{3'4'}$, relative to the thymine derivatives. These changes are larger for the -pT* units than for the Tp*- units. For example in -pT* of d(TpT*) the $J_{1'2'}$ coupling (3.7 Hz, 20°C) is the smallest such coupling observed in a 2′-deoxyriboside, while the magnitudes of $J_{2''3'}$ (6.8 Hz) and $J_{3'4'}$ (7.1 Hz) are the largest observed for these couplings. This pattern of changes indicates a shift away from the S-type of pucker which dominates in the thymidylyl residues. Overlooking any electronegativity corrections to the couplings, the *trans* couplings indicate a near balance of the N- and S- types of pucker in T*p- of d(T*pT) and a slight bias for S in T*p- of d(T*pT*). For the -pT* units of d(TpT*) and d(T*pT*), a bias towards the N-type

is evident ($J_{1'2'} < J_{2''3'} \approx J_{3'4'}$), with a 60–70% N population. Note also that the *trans* as well as *cis* couplings of the Tp*- and -pT* units are similar to those of 3′dT*MP and 5′dT*MP, respectively, indicating that no drastic change in conformation occurs upon incorporation of the monomers into the dimers. However, a greater preference for the N-pucker is apparent in -pT* of d(TpT*), relative to 5′dT*MP (compare *trans* couplings).

Also interesting is the similarity in the magnitudes of the sum, $J_{1'2'} + J_{3'4'}$, which lie in the range 10.4–11.2 Hz for the T derivatives (overall average, 10.7 Hz) and 10.5–11.4 Hz for the T* derivatives (overall average, 10.9 Hz), considering data for both the monomers and dimers. This would suggest that major differences in τ_m do not exist for the T and T* derivatives.[47] Note that in the crystal state the τ_m value of dT* is only 6.9° less than that of dT.[19]

Conformation About the C(4′)-C(5′) (ψ) Bond

The populations of the $g^+(\psi)$, $t(\psi)$, and $g^-(\psi)$ conformers (Fig. 1) can be estimated from the $J_{4'5'}$ and $J_{4'5''}$ data (Table V). For our calculations we have used the parameterization of Haasnoot et al.,[51] which corrects for electronegativity effects on the coupling constants. The calculated populations will differ (<10%) from those of earlier methods,[24] but the conformational trends predicted will be the same. In an earlier report on dT, dT*, and their monophosphates,[24] we noted that a *syn* base destabilizes $g^+(\psi)$, particularly at the 5′-monophosphate level. This destabilization of $g^+(\psi)$ is manifest in an increase in $\Sigma(J_{4'5'} + J_{4'5''})$. The prevailing trend (Table III) is to larger Σ values for the T*p- and -pT* units, relative to the Tp- and -pT units, and thus destabilization of $g^+(\psi)$ by the *syn* base occurs at the dimer level as well. Further trends in the ψ-bond conformations are now discussed.

Monomers

For the various thymine monomers, the $g^+(\psi)$ conformer dominates, whereas $g^-(\psi)$ is least favored. The trend in $\%g^+(\psi)$ is dT ≈ 3′dTMP < 5′dTMP < dpTp, with an overall change from 50 to 80% in the series. Thus, a 5′-phosphate enhances $\%g^+(\psi)$, which is further enhanced by the 3′-phosphate in dpTp. This contrasts with the theoretical finding[52] that a 3′-terminal phosphate stabilizes the $t(\psi)$ domain of the -pAp fragment of d(ApAp).

For the T* monomers, $t(\psi)$ rather than $g^+(\psi)$ is the favored conformer. Now the $\%g^+(\psi)$ follows the opposite trend, dT* ≈ 3′d*TMP > 5′T*MP > dpT*p, with an overall change from 35 to 21%. Ionization of the phosphate does not bring about large population changes in dpT*p or in dpTp. (Compare data at high and low pH.) It is interesting to note that whereas the 3′-phosphate stabilizes $g^+(\psi)$ in the *anti* series of molecules (compare 5′dTMP and dpTp), it stabilizes $t(\psi)$ in the *syn* series (compare 5′dT*MP and dpT*p).

TABLE V
Calculated Populations (%)[a] of the g^+, t, g^- Conformers of the C(4′)-C(5′)(ψ) and C(5′)-O(5′) (ϕ) Bonds

Molecule	Temp. (°C)	pH	C(4′)-C(5′)(ψ) g^+	t	g^-	C(5′)-O(5′)(ϕ) g^+	t	g^-
dT Residues								
dT	30	6.5	50	36	14	—	—	—
3′dTMP	30	5.0	53	35	12	—	—	—
5′dTMP	30	5.4	61	—	—	—	72	—
dpTp	20	4.5	79	—	—	—	76	—
	20	7.3	81	—	—	—	82	—
d(TpT)	20	6.5	57	27	16	—	—	—
d(TpT*)	20	6.5	61	35	4	—	—	—
	60	6.5	56	34	10	—	—	—
d(TpT)	20	6.5	75	27	−2	7	83	10
d(T*pT)	20	6.5	62	32	6	9	82	9
	60	6.5	57	35	8	14	75	11
dT* Residues								
dT*	30	6.5	35	54	11	—	—	—
3′dT*MP	18	6.0	35	47	18	—	—	—
5′dT*MP	25	6.0	30	48	22	17	65	18
dpT*p	20	3.7	25	64	11	20	60	20
	20	7.5	21	69	10	17	65	18
d(T*pT)	20	6.5	34	57	9	—	—	—
	60	6.5	35	53	11	—	—	—
d(T*pT*)	20	6.5	33	54	13	—	—	—
d(TpT*)	20	6.5	23	76	1	17	77	6
	60	6.5	23	71	6	19	68	13
d(T*pT*)	20	6.5	41	57	2	13	74	13

[a] Using $J_{4'5'}$, $J_{4'5''}$, $J_{5'P}$, and $J_{5''P}$ in Table III with parameterization of Ref. 51. Data for dT, dT*, 3′dTMP, 3′dT*MP, 5′dTMP, and 5′dT*MP from Ref. 24. Dimer data refer to the underlined residue.

Comparison of the data for corresponding monomers in the T and T* series (Table V) reveals the extent of the reduction in $\%g^+(\psi)$ brought about by the *syn* base. At the various levels the decreases are: deoxynucleoside (15%) ≈ 3′-monophosphate (18%) < 5′-monophosphate (30%) < 3′,5′-diphosphate (55–60%). One can attribute this destabilization of $g^+(\psi)$ to a repulsion between the 2-keto oxygen of the base and the 5′-oxygen that lies over the sugar ring in the $g^+(\psi)$ conformer. This interpretation is consistent with the greater decrease in $\%g^+(\psi)$ at the 5′-monophosphate and 3′,5′-diphosphate levels, but it is not clear why the populations are not affected by the ionization state of the phosphates (cf. data for the 3′,5′-diphosphates at the two pH values).

It is interesting to note that the decrease in $\%g^+(\psi)$ is greatly enhanced by the presence of the 3′-phosphate (cf. decreases at the 5′-monophosphate and 3′,5′-diphosphate levels) even though this group is on the *exo* side of the sugar ring. This must be a consequence of the apparent 3′-phosphate–5′-phosphate interaction, which in the case of the *anti* molecules

leads to an increase in $\%g^+(\psi)$ (cf. 5′dTMP and dpTp) and to a decrease in $\%g^+(\psi)$ in the case of the *syn* molecules (cf. 5′dT*MP and dpT*p). We think that this striking difference in the effect of 3′-phosphorylation is due to the differences in ring puckering in the *syn* and *anti* series. As noted above, the *syn* base brings about a shift towards the N-pucker, a consequence of which is a reduction in the average separation of the negative charges on the 3′- and 5′-phosphates. Should this reduction lead to a repulsion between the groups, then rotation from $g^+(\psi)$ [and $g^-(\psi)$] into $t(\psi)$ is expected, since this change increases the charge separation (Fig. 1). Support for this argument comes from an earlier study[26] of the ^{13}C-^{31}P coupling constants of the mono- and diphosphates. There it was shown that 5′-phosphorylation of 3′dT*MP (but not 3′dTMP) led to a shift from the g^- to the t conformation of the C3′-O3′ (ϕ) bond, another change which increases the separation of the 3′- and 5′-phosphates.

Dinucleoside Monophosphates

In general the conformational trends at the monomer level are retained at the dimer level (Table V). Thus, $g^+(\psi)$ and $t(\psi)$ dominate for the dT and dT* residues, respectively, whereas $g^-(\psi)$ is least populated in all instances. Incorporation of 3′dTMP and 3′dT*MP in a dimer, as Tp- or T*p units, respectively, has little effect (<10%) on ψ conformer distribution. This insensitivity is not surprising, since the terminal hydroxymethyl is not involved in the internucleotide linkage. Larger population redistributions are noted when 5′dTMP and 5′dT*MP are incorporated as -pT and -pT* fragments, respectively. For example, a 15% increase in $\%g^+(\psi)$ occurs when 5′dTMP is incorporated into d(TpT) [but not into d(T*pT)]. Incorporation of 5′dT*MP into d(TpT*) leads to a small (7%) decrease in $\%g^+(\psi)$ and a large decrease in $\%g^-(\psi)$ (21%). Noteworthy in the -pT* fragment of d(TpT*) is the large $\%t(\psi)$ (76%) and the vanishing small $\%g^-(\psi)$.

Relative to the Tp- units, the Tp*- units experience a large decrease in $\%g^+(\psi)$ (20–30%) and a comparable increase in $\%t(\psi)$, with much smaller changes in $\%g^-(\psi)$. The *syn* base effect is even larger for the -pT* unit of d(TpT*) [52% decrease in $\%g^+(\psi)$ and 49% increase in $\%t(\psi)$]. Free-energy calculations based on a population change of 50% indicate that in the presence of the *syn* base the $g^+(\psi)$ conformer is destabilized by about 1.3 kcal/mol relative to the energy of the $t(\psi)$ conformer. A smaller *syn* base effect is noted for the -pT* unit of d(T*pT*) [21% increase in $\%g^+(\psi)$; 25% increase in $\%t(\psi)$]. The reason for these differences in the -pT* units of d(TpT*) and d(T*pT*) is not obvious.

Conformation of the C3′-O3′(ϕ') Bond

Limited information about the conformation of the C3′-O3′(ϕ') bond (Fig. 1) can be obtained from the P3′-H3′ couplings (Table II). The $g^+(\phi')$ rotamer, which has never been observed in the crystal state, is generally ex-

TABLE V
Calculated Populations (%)[a] of the g^+, t, g^- Conformers of the C(4′)-C(5′)(ψ) and C(5′)-O(5′) (ϕ) Bonds

Molecule	Temp. (°C)	pH	C(4′)-C(5′)(ψ) g^+	t	g^-	C(5′)-O(5′)(ϕ) g^+	t	g^-
dT Residues								
dT	30	6.5	50	36	14	—	—	—
3′dTMP	30	5.0	53	35	12	—	—	—
5′dTMP	30	5.4	61	—	—	—	72	—
dpTp	20	4.5	79	—	—	—	76	—
	20	7.3	81	—	—	—	82	—
d(TpT)	20	6.5	57	27	16	—	—	—
d(TpT*)	20	6.5	61	35	4	—	—	—
	60	6.5	56	34	10	—	—	—
d(Tp**T**)	20	6.5	75	27	−2	7	83	10
d(T*p**T**)	20	6.5	62	32	6	9	82	9
	60	6.5	57	35	8	14	75	11
dT* Residues								
dT*	30	6.5	35	54	11	—	—	—
3′dT*MP	18	6.0	35	47	18	—	—	—
5′dT*MP	25	6.0	30	48	22	17	65	18
dpT*p	20	3.7	25	64	11	20	60	20
	20	7.5	21	69	10	17	65	18
d(**T***pT)	20	6.5	34	57	9	—	—	—
	60	6.5	35	53	11	—	—	—
d(**T***pT*)	20	6.5	33	54	13	—	—	—
d(Tp**T***)	20	6.5	23	76	1	17	77	6
	60	6.5	23	71	6	19	68	13
d(T*p**T***)	20	6.5	41	57	2	13	74	13

[a] Using $J_{4'5'}$, $J_{4'5''}$, $J_{5'P}$, and $J_{5''P}$ in Table III with parameterization of Ref. 51. Data for dT, dT*, 3′dTMP, 3′dT*MP, 5′dTMP, and 5′dT*MP from Ref. 24. Dimer data refer to the underlined residue.

Comparison of the data for corresponding monomers in the T and T* series (Table V) reveals the extent of the reduction in $\%g^+(\psi)$ brought about by the *syn* base. At the various levels the decreases are: deoxynucleoside (15%) ≈ 3′-monophosphate (18%) < 5′-monophosphate (30%) < 3′,5′-diphosphate (55–60%). One can attribute this destabilization of $g^+(\psi)$ to a repulsion between the 2-keto oxygen of the base and the 5′-oxygen that lies over the sugar ring in the $g^+(\psi)$ conformer. This interpretation is consistent with the greater decrease in $\%g^+(\psi)$ at the 5′-monophosphate and 3′,5′-diphosphate levels, but it is not clear why the populations are not affected by the ionization state of the phosphates (cf. data for the 3′,5′-diphosphates at the two pH values).

It is interesting to note that the decrease in $\%g^+(\psi)$ is greatly enhanced by the presence of the 3′-phosphate (cf. decreases at the 5′-monophosphate and 3′,5′-diphosphate levels) even though this group is on the *exo* side of the sugar ring. This must be a consequence of the apparent 3′-phosphate–5′-phosphate interaction, which in the case of the *anti* molecules

leads to an increase in $\%g^+(\psi)$ (cf. 5′dTMP and dpTp) and to a decrease in $\%g^+(\psi)$ in the case of the *syn* molecules (cf. 5′dT*MP and dpT*p). We think that this striking difference in the effect of 3′-phosphorylation is due to the differences in ring puckering in the *syn* and *anti* series. As noted above, the *syn* base brings about a shift towards the N-pucker, a consequence of which is a reduction in the average separation of the negative charges on the 3′- and 5′-phosphates. Should this reduction lead to a repulsion between the groups, then rotation from $g^+(\psi)$ [and $g^-(\psi)$] into $t(\psi)$ is expected, since this change increases the charge separation (Fig. 1). Support for this argument comes from an earlier study[26] of the ^{13}C-^{31}P coupling constants of the mono- and diphosphates. There it was shown that 5′-phosphorylation of 3′dT*MP (but not 3′dTMP) led to a shift from the g^- to the t conformation of the C3′-O3′ (ϕ) bond, another change which increases the separation of the 3′- and 5′-phosphates.

Dinucleoside Monophosphates

In general the conformational trends at the monomer level are retained at the dimer level (Table V). Thus, $g^+(\psi)$ and $t(\psi)$ dominate for the dT and dT* residues, respectively, whereas $g^-(\psi)$ is least populated in all instances. Incorporation of 3′dTMP and 3′dT*MP in a dimer, as Tp- or T*p units, respectively, has little effect (<10%) on ψ conformer distribution. This insensitivity is not surprising, since the terminal hydroxymethyl is not involved in the internucleotide linkage. Larger population redistributions are noted when 5′dTMP and 5′dT*MP are incorporated as -pT and -pT* fragments, respectively. For example, a 15% increase in $\%g^+(\psi)$ occurs when 5′dTMP is incorporated into d(TpT) [but not into d(T*pT)]. Incorporation of 5′dT*MP into d(TpT*) leads to a small (7%) decrease in $\%g^+(\psi)$ and a large decrease in $\%g^-(\psi)$ (21%). Noteworthy in the -pT* fragment of d(TpT*) is the large $\%t(\psi)$ (76%) and the vanishing small $\%g^-(\psi)$.

Relative to the Tp- units, the Tp*- units experience a large decrease in $\%g^+(\psi)$ (20–30%) and a comparable increase in $\%t(\psi)$, with much smaller changes in $\%g^-(\psi)$. The *syn* base effect is even larger for the -pT* unit of d(TpT*) [52% decrease in $\%g^+(\psi)$ and 49% increase in $\%t(\psi)$]. Free-energy calculations based on a population change of 50% indicate that in the presence of the *syn* base the $g^+(\psi)$ conformer is destabilized by about 1.3 kcal/mol relative to the energy of the $t(\psi)$ conformer. A smaller *syn* base effect is noted for the -pT* unit of d(T*pT*) [21% increase in $\%g^+(\psi)$; 25% increase in $\%t(\psi)$]. The reason for these differences in the -pT* units of d(TpT*) and d(T*pT*) is not obvious.

Conformation of the C3′-O3′(ϕ') Bond

Limited information about the conformation of the C3′-O3′(ϕ') bond (Fig. 1) can be obtained from the P3′-H3′ couplings (Table II). The $g^+(\phi')$ rotamer, which has never been observed in the crystal state, is generally ex-

cluded in any analysis. But no preference for either the $t(\phi')$ or $g^-(\phi')$ conformer can be determined from $J_{P3'}$, since the coupled nuclei are *gauche* in each. However, increases in $J_{P3'}$ can be attributed to a trend towards the $\phi' = -120°$ situation (P3′-H3′ eclipsed). A large coupling (9.8 Hz) is observed for dpT*p (pH = 7.5). On the other hand, $J_{P3'}$ is relatively small in Tp- of d(TpT), indicating a trend away from the eclipsed orientation. The magnitudes of the other $J_{P3'}$ entries are intermediate and show no clear differences for the T and T* derivatives. [On occasion, dihedral angles have been calculated from the $J_{P3'}$ couplings and assigned to the $g^-(\phi')$ and $t(\phi')$ conformers; the works of Jardetzky[53] and Wildman[54] suggest that these calculated angles may be devoid of meaning.]

The pair of ^{13}C-^{31}P couplings involving P3′ and C2′ and C4′ provide more information about the ϕ' conformational situation. The data for the 3′-monophosphates and 3′,5′-diphosphates have been discussed[26]; a discussion of the dimer data is in preparation. In summary, however, these measurements indicate a preference for the $t(\phi')$ conformation in all of our 3′-nucleotidyl units, with some dependence on the nature of the base.

Conformation About the C(5′)-O(5′)(ϕ) Bond

Estimates of the populations of the $g^+(\phi)$, $t(\phi)$, and $g^-(\phi)$ conformers of a 5′-nucleotidyl unit can be obtained from the $J_{5'P}$ and $J_{5''P}$ couplings (Table V). The ϕ-bond populations show smaller variation than those of the ψ bond. In all cases the $t(\phi)$ conformer dominates (60–82%), in line with earlier studies on other 5′-nucleotides and oligonucleotides.[24,34–40] There are prevailing trends toward a decrease in $\%t(\phi)$ with the *anti*-to-*syn* base change. The reduction in $\%t(\phi)$ in the *syn* units is probably not due to a direct effect of the base, but is more likely a consequence of the reduction in the $g^+(\psi)$. This ψ-ϕ interdependence has been discussed elsewhere.[34,55]

Base Stacking and Photodimer Formation

Molecular models reveal that each of the four dimers, d(TpT), d(T*pT), d(TpT*), and d(T*pT*), with the T and T* bases in their favored *anti* and *syn* conformations, respectively, can be folded into a right-hand base-stacked conformation. Thus, there seems to be no reason to discount stacking by a *syn* pyrimidine, whether it be on the 3′- or 5′-linked residue. The isolation, from uv-irradiated DNA[14] and d(TpT),[56] of a *minor* thymine photodimer product with the *TRANS–SYN* cyclobutane geometry[15] seems to provide experimental evidence for a base stack involving a *syn* thymine base. The *CIS–SYN* product undoubtedly arises from a right-handed base-stacked d(TpT) fragment in which both bases are *anti*; rotation of the thymine on the 3′-linked residue into the *syn* conformation would seem to lead to the minor, *TRANS–SYN* product. However, it is conceivable that the *TRANS–SYN* product could be generated from a d(TpT) fragment

in which the P-O3′(ω') and P-O5′(ω) bonds are oriented g^+ rather than g^-, as in the right-hand stack. In this g^+g^+ orientation, partial overlap of the thymine bases is possible, but their orientation is such that the *TRANS–SYN* cyclobutane ring would be generated by irradiation. The presence of the g^+g^+ orientation in dinucleoside monophosphates has been inferred from ^{1}H-nmr data.[57]

Since the formation of the cyclobutane photoproducts requires the approach of the C5-C6 bonds of the bases involved, studying this photoreaction provides information about the conformations accessible to a dimer fragment. Thus, we have subjected d(TpT*), d(T*pT), and d(T*pT*) to uv irradiation using the procedure of Johns et al.[56] Details of the experiments will be published later. Preliminary ^{1}H-nmr studies at 360 MHz revealed photodimer formation from d(T*pT) (at least one product) and from d(T*pT*) (two products in a 5:4 ratio). None were obtained from d(TpT*), even after 14 h of irradiation in the presence of photosensitizer (acetophenone).[17] In part, these observations seem consistent with model building. Thus, both d(T*pT) and d(T*pT*), with their T and T* units in the *anti* and *syn* conformations, respectively, can be folded into a right-hand stack which brings their C5-C6 bonds into proximity. The presence of multiple products will remain difficult to explain until we have been able to separate the individual products. However, this observation seems to suggest alternate conformations which bring the C5-C6 bonds into proximity (involving perhaps a *syn* T or *anti* T* or a g^+g^+ folded dimer).

The absence of d(TpT*) photoproducts also seems reasonable, since the C5-C6 bonds are distant in a right-hand stack (and in the g^+g^+ conformer with partial base overlap) (Fig. 3).

Most likely the right-hand d(T*pT) stack is the precursor of a d(T*[p]T) photoproduct (square brackets about p designate a cyclobutane ring[15]) having the *TRANS–SYN* geometry. Overlooking the positions of the methyl groups, we predict that this product will be shown to resemble the minor, *TRANS–SYN* d(T[p]T) product. On the other hand, the g^-g^- stacked conformation of d(T*pT*) leads most likely to a *CIS–SYN* d(T*[p]T*) product. Again, overlooking the positions of the methyl groups, we predict that this product will be shown to be *configurationally distinguishable* from the major, *CIS–SYN* d(T[p]T) product by the different mode of attachment of the bases to their sugar residues (Fig. 3).

The formation of photodimers provides evidence that d(T*pT) and d(T*pT*) can be folded into a conformation involving base overlap, while the absence of photoproducts of d(TpT*) indicates, at most, that the C5-C6 bonds are not appropriately oriented for photoreaction in any folded form accessible to this dimer. These studies, however, provide no information about the extent to which the folded forms occur. It is also unfortunate that the conventional nmr method of detecting base interaction (measurements of the temperature dependence of the base-proton chemical shifts) is seriously limited for our molecules, since only small ring currents are induced in pyrimidine rings.

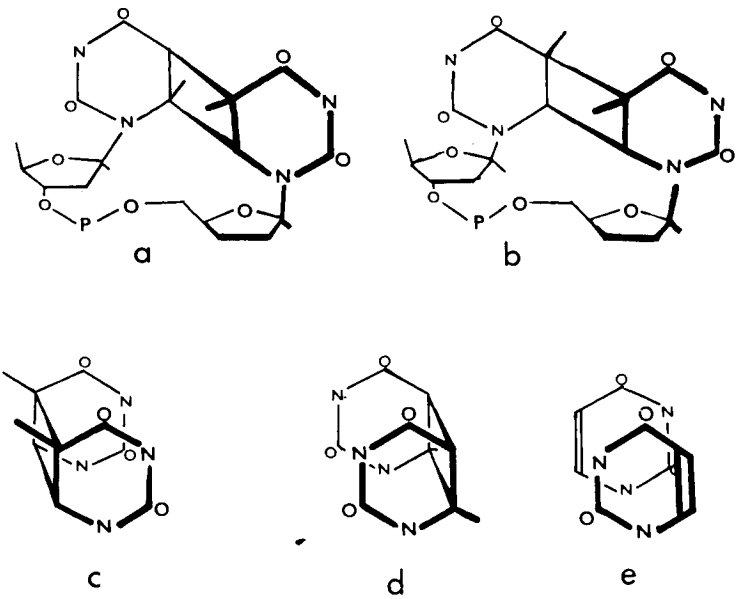

Fig. 3. (a and b) Structure of the *TRANS–SYN* cyclobutane photoproducts expected to result from uv-irradiation of d(T*pT) (a) and d(TpT) (b) folded into right-handed base-stacked conformations, with their 3′-linked and 5′-linked residues in the *syn* and *anti* conformations about their *N*-glycosyl linkage, respectively. The fully capitalized *TRANS–SYN* refers to the cyclobutane geometry (Ref. 15); the lower-case *syn* and *anti* refer to the *N*-glycosyl conformation. (c and d). The *CIS–SYN* cyclobutane photodimers expected from (c) *d*(TpT) (right-hand stack, both residues *anti*) and (d) d(T*pT*) (right-hand stack, both residues *syn*). (e) Overlap of the pyrimidine bases in a right-hand base-stacked conformation of d(TpT*), viewed from the 5′-linked residue to the 3′-linked residue. The back base is *anti*; the front base is *syn*. In (c)–(e) the sugar–phosphate backbone (not shown) is aligned as in (a) and (b).

However, some of the chemical shift data (Table I) seem to point to base stacking in d(TpT*). In space-filling models of this dimer folded into a right-hand stack, the 2-keto oxygen of the *syn* T* base lies near to the H2′ and H2″ protons of the Tp- unit. (Folding of the dimers also alters the disposition of this H2″ relative to the ester O5′ and nonester O atoms on the phosphorus). Hence, if the -pT unit of d(TpT) is replaced by a -pT* unit, then H2′ and H2″ of the Tp- unit should experience chemical-shift changes, provided that significant right-hand folding occurs. To test this for the Tp- unit of d(TpT*), we calculate the $\Delta\delta$ values, defined as the chemical shift of a proton in this unit relative to its resonant position in Tp- of d(TpT). At 20°C these are (in ppm): H1′ (0.06), H2′ (−0.10), H2″ (−0.13), H3′ (0.01), H4′ (−0.03), H5′ (0.03), H5″ (0.00), H6 (−0.11), and CH_3 (0.02), with positive values indicating a downfield shift. Thus, substantial shifts are experienced by H2′ and H2″ as well as by H6 and H1′, which are near to the contact surfaces of the stacked bases. The remaining, distant protons experience shifts of 0.03 ppm or less. If these $\Delta\delta$ values are related to base-stacking phenomena, then they are expected to decrease

at elevated temperatures. Using the 65°C data for d(TpT)[36] and the 60°C data for d(TpT*), we find a reduction in $\Delta\delta$ to 0.00 ppm (H1′), −0.04 ppm (H2′), −0.09 ppm (H2″), and −0.07 ppm (H6), with the other $\Delta\delta$ values at <0.02 ppm.

Though these chemical-shift data and the photoproduct formation provide very qualitative information, they do indicate that the question of the stacking of *syn* pyrimidine bases warrants further investigation.

Syn Pyrimidines in Double Helices

The *syn* T* (or *syn* T) base cannot be incorporated into the conventional double helix with Watson-Crick hydrogen bonding. However, to test whether other double helices are accessible to this *syn* base, we have built molecular models of self-complementary A(adenosine)-T* (and A-T) copolymers, such as AT*AT*AT*. With the purine and pyrimidine bases in their *anti* and *syn* forms, respectively, an antiparallel right-handed double helix can be assembled with Hoogsteen hydrogen bonds between the A and T* (or T) bases. (This bonding scheme, which involves N6-H and N7 of the A base and the O4 and N3-H atoms of T*, has been observed in cocrystals of adenine and uracil derivatives.[58] The involvement of Hoogsteen bonding, involving *anti* thymine bases, has been suggested[59] for certain multistranded complexes.) We hope to test for such putative duplexes with synthetic A-T* oligonucleotides; the dimer d(ApT*) is now available. Encouraging are the theoretical calculations[60] which indicate that the energy of the Hoogsteen bonding is larger than that of the Watson-Crick bonding. It is also interesting to note that our novel right-handed helix resembles the left-handed Z-DNA[1] in that, relative to B-DNA, the base pairs are more exposed and the phosphates are closer together. Also, only one, shallow groove appears in Z-DNA and in our double helix.

SUMMARY

Proton magnetic resonance data have been obtained for a series of derivatives of 2′-deoxythymidine (dT) and 6-methyl-2′-deoxyuridine (dT*), including the 3′,5′-diphosphates, dpTp and dpT*p, and four dideoxynucleoside monophosphates, d(TpT), d(TpT*), d(T*pT), and d(T*pT*). The data are compared with earlier results on dT, dT*, and their 3′- and 5′-monophosphates. The results reveal that the dT* units prefer the *syn* conformation about the *N*-glycosyl linkage, contrasting with the preference for *anti* in the dT units. Coupling-constant data indicate a trend towards eclipsing of the substituents on the C1′-C2′-C3′ fragment of the dT* residues. Using crystallographic data for dT and dT*, this trend is rationalized in terms of an N $\rightleftarrows$ S model in which both modes of pucker are biased towards O4′-*endo* in the dT* units relative to the dT units. The presence of the *syn* base leads to a destabilization of the g^+ conformer about C4′-C5′, leading to an increase in the *t* conformer. Photodimer formation and

chemical-shift data indicate that base-stacked conformations are accessible to dimers containing the *syn* dT* unit. Model building reveals that a *syn* T* (or *syn* T) base can be incorporated into an antiparallel, right-handed double helix with Hoogsteen hydrogen bonds between the A and T* (or T) bases.

This work was supported by operating grants from NSERC (Canada). W. P. Niemczura is grateful for a Manitoba Fellowship. We acknowledge Dr. J. L. Markley, The Biochemical Magnetic Resonance Laboratory, Purdue University (NIH Grant RR-01077), for the 360-MHz spectra; Dr. A. A. Bothner-by, The NMR Facility for Biomedical Studies, The Carnegie-Mellon University (NIH Grant RR00292), for the 600-MHz spectra; and Dr. W. A. Gibbons, The University of Wisconsin, Madison (NIH Grant AM-18604 and NSF PCM 79/13976), for the 270-MHz spectra. We thank R. Sebastian and W. Blonski for the analysis of the 600-MHz spectra.

References

1. Wang, A. H.-J., Quigley, G. J., Kolpak, F. J., Crawford, J. L., Van Boom, J. H., van der Marel, G. & Rich A. (1979) *Nature* **282,** 680–686.

2. Arnott, S., Chandrasekaran, R., Birdsall, D. L., Leslie, A. G. W. & Ratliff, R. L. (1980) *Nature* **283,** 743–745.

3. Saenger, W. & Scheit, K. H. (1970) *J. Mol. Biol.* **50,** 153–169.

4. Hart, P. A. & Davis, J. P. (1971) *J. Am. Chem. Soc.* **93,** 753–760.

5. Nanda, R. K., Tewari, R., Govil, G. & Smith, I. C. P. (1974) *Can. J. Chem.* **53,** 371–375.

6. Lavallee, D. K. & Coulter, C. L. (1973) *J. Am. Chem. Soc.* **95,** 576–581.

7. Neumann, J. M., Borrel, J., Thiery, J. M., Guschlbauer, W. & Tran-Dinh, S. (1977) *Biochem. Biophys. Acta* **479,** 427–440.

8. Chachaty, C., Yokono, T., Tran-Dinh, S. & Guschlbauer, W. (1977) *Biophys. Chem.* **6,** 151–159.

9. Markham, A. F., Uesugi, S., Ohtuska, E. & Ikehara, I. (1979) *Biochemistry*, **18,** 4936–4942.

10. Markham, A. F., Nakagawa, E., Ohtuska, E. & Ikehara, I. (1980) *Biopolymers* **19,** 285–296.

11. Hurd, R. E. & Reid, B. R. (1977) *Nucleic Acid. Res.* **4,** 2747–2755.

12. Pullman, B. & Berthod, H. (1973) *Proceedings of the International Symposium on the Conformation of Biological Molecules and Polymers, Symposia on Quantum Chemistry and Biochemistry*, Vol. 5, Pullman, B. & Bergman, E. D., Eds., Academic Press, New York, pp. 209–224.

13. Yathindra, N. & Sundaralingam, M. (1974) *Biopolymers* **13,** 2061–2076.

14. Ben-Hur, E. & Ben-Ishai (1968) *Biochim. Biophys. Acta* **166,** 9–15.

15. Cohn, W. E., Leonard, N. J. & Wang, S. Y. (1974) *Photochem. Photobiol.* **19,** 89–94.

16. Hruska, F. E., Wood, D. J., Ogilvie, K. K. & Charlton, J. L. (1975) *Can. J. Chem.* **53,** 1193–1203.

17. Liu, F.-T. & Yang, N. C. (1978) *Biochemistry* **17,** 4865–4876.

18. Suck, D., Saenger, W. & Vorbruggen, V. (1972) *J. Am. Chem. Soc.* **94,** 6520–6526.

19. Birnbaum, G. I., Hruska, F. E. & Niemczura, W. P. (1980) *J. Am. Chem. Soc.* **102,** 5586–5590.

20. Miles, D. W., Robins, M. J., Robins, R. K., Winkley, M. W. & Eyring, H. (1969) *J. Am. Chem. Soc.* **91,** 824–831.

21. Miles, D. W., Robins, M. J., Robins, R. K., Winkley, M. W. & Eyring H. (1969) *J. Am. Chem. Soc.* **91,** 831–838.

22. Schweizer, M. P., Banta, E. B., Witkowski, J. T. & Robbins, R. K. (1973) *J. Am. Chem. Soc.* **95,** 3770–3778.

23. Cadet, J., Ducolomb, R. & Taieb, C. (1975) *Tetrahedron Lett.*, 3455–3458.

24. George, A. L. Hruska, F. E., Ogilvie, K. K. & Holy, A. (1978) *Can. J. Chem.* **56,** 1170–1176.
25. Cadet, J., Taieb, C., Remin, M., Niemczura, W. P. & Hruska, F. E. (1980) *Biochim. Biophys. Acta* **608,** 435–445.
26. Niemczura, W. P. & Hruska, F. E. (1980) *Can. J. Chem.* **58,** 472–478.
27. Holy, A. (1973) *Coll. Czech. Chem. Commun.* **39,** 3374–3382.
28. Holy, A. (1973) *Tetrahedron Lett.*, 1147–1150.
29. Stawinski, J., Hozumi, T., Narang, S. A., Bahl, C. P. & Wu, R. (1977) *Nucleic Acid Res.* **4,** 353–371.
30. Cozzone, P. J. & Jardetzky, O. (1976) *Biochemistry* **15,** 4860–4865.
31. Glascoe, P. K. & Long, F. A. (1960) *J. Phys. Chem.* **64,** 188–190.
32. Haigh, C. W. & Williams, J. M. (1969) *J. Mol. Spectrosc.* **32,** 398–406.
33. W. P. Niemczura (1980), Ph.D. thesis, The University of Manitoba.
34. Davies, D. B. (1978) *Prog. Nucl. Magn. Reson. Spectrosc.* **12,** 135–225, and references therein.
35. Davies, D. B. & Danyluk, S. S. (1974) *Biochemistry* **13,** 4417–4434.
36. Wood, D. J., Hruska, F. E. & Ogilvie, K. K. (1974) *Can. J. Chem.* **52,** 3353–3366.
37. Wood, D. J., Ogilvie, K. K. & Hruska, F. E. (1975) *Can. J. Chem.* **53,** 2781–2790.
38. Altona, C., Van Boom, J. H. & Haasnoot, C. A. G. (1976) *Eur. J. Biochem.* **71,** 557–562.
39. Cheng, D. M. & Sarma, R. H. (1977) *J. Am. Chem. Soc.* **99,** 7333–7345.
40. Cheng, D. M., Dhingra, M. M. & Sarma, R. H. (1978) *Nucleic Acid Res.* **5,** 4399–4416.
41. Fang, K. N., Kondo, N. S., Miller, P. S. & Ts'o, P. O. P. (1971) *J. Am. Chem. Soc.* **93,** 6647–6656.
42. Fraser-Reid, B. and Radatus, B. (1971) *J. Am. Chem. Soc.* **93,** 6342–6344.
43. Remin, M. & Shugar, D. (1972) *Biochem. Biophys. Res. Commun.* **48,** 636–642.
44. Ritchie, R. G. S. & Perlin, A. S. (1977) *Carbohydrate Res.* **55,** 121–128.
45. Young, D. W., Tollin, P. & Wilson H. R. (1969) *Acta. Crystallogr.* **25,** 1423–1432.
46. Giessner-Prettre, C. & Pullman, B. (1977) *J. Theor. Biol.* **65,** 171–188.
47. Altona, C. & Sundaralingam, M. (1973) *J. Am. Chem. Soc.* **95,** 2333–2344.
48. Altona, C. & Sundaralingam, M (1972) *J. Am. Chem. Soc.* **94,** 8205–8212.
49. Lavallee, D. K. & Myers, R. B. (1978) *J. Am. Chem. Soc.* **100,** 3907–3912.
50. Remin, M., Ekiel, I. & Shugar, D. (1975) *Eur. J. Biochem.* **53,** 197–206.
51. Haasnoot, C. A. G., de Leeuw, F. A. A. M., de Leeuw, H. P. M. & Altona, C. (1979) *Recl. Trav. Chim. Pays Bas* **98,** 576–577.
52. Broyde, S. & Hingerty B. (1979) *Nucleic Acid Res.* **6,** 2165–2178.
53. Jardetzky, O. (1980) *Biochim. Biophys. Acta* **621,** 227–232.
54. Wildman, T. A. (1980) *Chem. Phys. Lett.* **75,** 383–387.
55. Wood, D. J., Mynott, R. J., Hruska, F. E. & Sarma, R. H. (1973) *FEBS Lett.* **34,** 323–326.
56. Johns, H. E., Pearson, M. L., LeBlanc, J. C. & Helleiner, C. W. (1964) *J. Mol. Biol.* **9,** 503–524.
57. Ezra, F. S., Lee, C. H., Kondo, N. S., Danyluk, S. S. & Sarma, R. H. (1977) *J. Am. Chem. Soc.* **16,** 1977–1987.
58. Hoogsteen, K. (1963) *Acta Crystallogr.* **16,** 907–916.
59. Johnson, D. & Morgan, A. R. (1978) *Proc. Natl. Acad. Sci. (USA)* **75,** 1637–1641.
60. Pullman, B. & Pullman, A. (1969) *Prog. Nucleic Acid Res. Mol. Biol.* **9,** 327–402.

Received November 4, 1980
Accepted February 20, 1981